



Published in final edited form as:

Biochemistry. 2018 March 20; 57(11): 1681–1684. doi:10.1021/acs.biochem.8b00061.

Surface Charge Modulates Protein–Protein Interactions in Physiologically Relevant Environments

Alex J. Guseman[†], Shannon L. Speer[†], Gerardo M. Perez Goncalves[†], and Gary J. Pielak^{*,†,‡,§,||}

[†]Department of Chemistry, University of North Carolina at Chapel Hill, Chapel Hill, North Carolina 27599, United States

[‡]Department of Biochemistry and Biophysics, University of North Carolina at Chapel Hill, Chapel Hill, North Carolina 27599, United States

[§]Lineberger Comprehensive Cancer Center, University of North Carolina at Chapel Hill, Chapel Hill, North Carolina 27599, United States

^{||}Integrative Program for Biological and Genome Sciences, University of North Carolina at Chapel Hill, Chapel Hill, North Carolina 27599, United States

Abstract

Protein–protein interactions are fundamental to biology yet are rarely studied under physiologically relevant conditions where the concentration of macromolecules can exceed 300 g/L. These high concentrations cause cosolute–complex contacts that are absent in dilute buffer. Understanding such interactions is important because they organize the cellular interior. We used ¹⁹F nuclear magnetic resonance, the dimer-forming A34F variant of the model protein GB1, and the cosolutes bovine serum albumin (BSA) and lysozyme to assess the effects of repulsive and attractive charge–charge dimer–cosolute interactions on dimer stability. The interactions were also manipulated via charge-change variants and by changing the pH. Charge–charge repulsions between BSA and GB1 stabilize the dimer, and the effects of lysozyme indicate a role for attractive interactions. The data show that chemical interactions can regulate the strength of protein–protein interactions under physiologically relevant crowded conditions and suggest a mechanism for tuning the equilibrium thermodynamics of protein–protein interactions in cells.

*Corresponding Author: Department of Chemistry, University of North Carolina at Chapel Hill, Chapel Hill, NC 27599-3290. gary_pielak@unc.edu. Phone: (919) 962-4495.

Author Contributions

A.J.G. and S.L.S. contributed equally to this work.

ORCID

Gary J. Pielak: 0000-0001-6307-542X

Notes

The authors declare no competing financial interest.

Supporting Information

The Supporting Information is available free of charge on the ACS Publications website at DOI: 10.1021/acs.biochem.8b00061. Materials and methods, predicted protein charges at pH 6.2, 6.8, and 7.5 (Table S1), charges of A34F variants as a function of pH (Figure S1), A34F GB1 structure (Figure S2), and protein cosolute charges as a function of pH (Figure S3) (PDF)

The formation and dissociation of protein complexes regulate processes ranging from signaling to transcription and metabolism, all of which are essential to maintaining cellular homeostasis.¹ Traditionally, these interactions were studied in a dilute buffered solution. In their native cellular environments, however, the concentration of macromolecules can exceed 300 g/L.^{2,3} These high concentrations of macromolecules are the source of the contacts that organize the cytoplasm.^{4,5} These interactions, which define quinary structure,^{6–8} comprise two components: hard-core steric repulsions and “soft” chemical interactions.⁹ Their influence is currently being investigated in the context of protein folding and stability.^{9–17} Here, we shift the emphasis to protein–protein interactions.^{18–20}

There have been more than three decades of speculation about how crowding influences the stability of a test protein.^{21–24} Originally, crowding effects were attributed solely to hard-core repulsions, which occur at short crowder–test protein distances, because of the large and unfavorable energy associated with the interpenetration of electron shells.⁹ Hard-core repulsions favor compact states. The stabilization from synthetic polymers was attributed to these repulsions, because the folded state occupies less space than the unfolded ensemble does. Results from early studies of protein dimerization under crowded conditions using inert polymers suggest that hard-core repulsions play but a small role in dimerization.²⁵ The minor increase in stability can be explained by the small decrease in volume when two monomers become a dimer.

Synthetic polymers, although traditionally used to simulate the crowded cellular environment, are a poor representation of biology, because they do not have the same surface properties as biological macromolecules.^{26,27} These so-called “soft” interactions include charge–charge contacts, hydrogen bonding, and hydrophobic interactions between the surface of a test protein and physiologically relevant crowded environments,^{9,28–34} but even synthetic polymers have chemical interactions with test proteins.^{27,35,36}

Nevertheless, hard-core repulsions are always present, and they are stabilizing when the products of a reaction occupy less space than the reactants do. The use of proteins and cellular lysates as cosolutes revealed the importance of chemical interactions, because globular proteins are destabilized in these environments despite the stabilizing effects of hard-core repulsions.^{19,30,37} In these environments, side chains and the exposed backbone on the surface of the test protein interact with the whole surface of the macromolecules [as opposed to specific (i.e., ligand) binding, which would be stabilizing]. The current model used to explain crowding effects predicts that chemical interactions stabilize proteins when repulsive and destabilize proteins when attractive. Extending this idea to protein–protein interactions, where hard-core repulsions are less important,²⁵ suggested to us that soft interactions can tune the protein complex stability.

We used a model homodimer system, the A34F variant of the B1 domain of protein G, GB1 (6 kDa, pI 4.5),^{38,39} to test this idea. Dimerization is driven by displacement of the Tyr-33 side chain from the hydrophobic core by the phenylalanine side chain at position 34. To compensate, the C-terminus of the α -helix unravels, forming a hydrophobic pocket for the Tyr-33 from a second molecule. The interaction is stabilized by hydrogen bonding between antiparallel β -strands at the dimer interface. The components of the 12 kDa homodimer

retain the tertiary structure of the monomer, forming a dimer resembling kissing spheres. As a variant of a thermostable monomer, the A34F variant provides access to nearly all GB1 variants in the Protherm database,⁴⁰ allowing us to control its surface properties.

We measured dimer stability in several cosolutes using ¹⁹F nuclear magnetic resonance (NMR). Fluorine is easily incorporated by supplementing minimal medium with 3-fluorotyrosine prior to inducing GB1 expression. Spectra of the purified protein show two resonances in slow exchange on the NMR time scale, allowing the monomer–dimer equilibrium to be determined from their areas.¹⁹ Dimer stability is minimally influenced by 100 g/L concentrations of the neutral synthetic polymers, but more influenced by protein cosolutes, suggesting a role for charge–charge interactions. We showed previously that attractive electrostatic interactions can be diminished by increasing the ionic strength.³⁰ Here, we examine the effect of electrostatics by manipulating the charge on GB1, by changing the charge of the cosolute proteins, and by manipulating the pH.

The A34F monomer has a charge of -4 at pH 7.5, and there are no groups that ionize from pH 7.5 to 6.2, the range used here (Figure S1). The charge on GB1 was changed by altering aspartic acid 40, which forms part of an acid patch on the surface remote from the dimer interface (Figure 1A and Figure S2). The D40N and D40K variants result in a $+1$ and $+2$ charge change with respect to the charge of the monomer. We refer to these proteins as A34F⁻⁴, A34F;D40N⁻³, and A34F;D40K⁻².

High concentrations of globular proteins have been used to mimic cellular conditions.^{10,12,30,41} The charge on the surroundings can be altered by using bovine serum albumin (BSA, 66 kDa, pI 4.5) and hen egg white lysozyme (14 kDa, pI 9.7) as cosolutes. Both proteins are highly soluble and commercially available in pure form but have different surfaces. At physiologically relevant pH values, BSA is a polyanion whereas lysozyme is a polycation (Figure S3). We used these proteins to create repulsive and attractive interactions with GB1.

We altered the charge on the protein cosolutes by controlling the pH. The net charge on BSA changes from -18 at pH 7.5 to -12 at pH 6.8 and -4 at pH 6.2 (Table S1 and Figure S3). The net charge on lysozyme changes from $+7$ at pH 7.5 to $+8$ at pH 6.8 and $+9$ at pH 6.2.

We first examined dimer stability in buffer at pH 7.5 and 298 K. $\Delta G_{D \rightarrow M}^{0'}$ increases from 5.8 to 6.4 kcal/mol for both A34F;D40N⁻³ and A34F;D40K⁻² (Table 1 and Figure 2). NMR data indicate that A34F;D40N⁻³ and A34F;D40K⁻² retain the structure of A34F⁻⁴ (Figure 1B,C). These data are consistent with the idea that stabilization arises from the mutation-induced decrease in intermonomer charge–charge repulsion (Figure S2), although we do not fully understand why the A34F;D40N⁻³ and A34F;D40K⁻² dimers have the same stability.

We have shown that 100 g/L BSA and 50 g/L lysozyme affect A34F⁻⁴ dimer stability at pH 7.5,¹⁹ and that under crowded conditions, charge–charge interactions become weaker at high ionic strengths.³⁰ BSA has a charge of -18 at this pH. Therefore, we expected, and observed (Table 1 and Figure 2), stabilization via electrostatic repulsions when polyanionic A34F is surrounded by polyanionic BSA. The net charge on lysozyme is $+7$ at pH 7.5. As expected

(Table 1), attractive electrostatic interactions between A34F and lysozyme destabilize the dimer.

To elucidate further the role of electrostatics, we investigated A34F⁻⁴ dimerization in BSA as a function of pH (Figure 3). As discussed above, the charge on the dimer does not change over our pH range, but the charge on the protein cosolutes does (Table S1). If electrostatic interactions between A34F⁻⁴ proteins and BSA are important, then the stabilizing effect of BSA should diminish with a decrease in pH, because of the decrease in repulsion between the dimer and BSA as BSA gains protons. Supporting this prediction, the stabilization decreases from 0.48 ± 0.06 kcal/mol at pH 7.5 to 0.31 ± 0.04 at pH 6.8 and 0.06 ± 0.04 kcal/mol at pH 6.2. These results and those from the charge-change variants suggest that the charges of both GB1 and BSA are responsible for the repulsive electrostatic interactions that stabilize the dimer, supporting the idea of a key role for charge-charge repulsion.

If the charge of the environment is important for dimer formation, we expect that as the cationic nature of lysozyme increases, the strength of attractive chemical interactions with GB1 will increase, resulting in destabilization. The stability of the dimer in lysozyme relative to its stability in buffer decreases with a decrease in pH from 7.5 to 6.8, but the value at pH 6.8 is within the uncertainty of that measured for lysozyme at pH 7.5. At pH 6.2, however, the decrease is larger (-0.31 ± 0.03 kcal/mol), showing that as the positive charge on lysozyme increases the strength of destabilizing attractive interactions increases.

Consistent with the results from the charge-change variants in buffer, there is no increase in destabilization in lysozyme with a change in the charge of GB1 from -3 to -2 (Table 1). Nevertheless, stability decreases when lysozyme is more cationic, suggesting an electrostatic role in destabilization. Other attractive interactions, e.g., hydrophobic contacts, polar interactions, and hydrogen bonds, likely also contribute to destabilization of the dimer, and the same effect is observed for the stability of an SH3 domain in lysozyme at pH 3 where lysozyme was destabilizing despite the existence of net charge-charge repulsion.³⁰

The charge-change variants were then tested in protein cosolutes at pH 7.5. Given the polyanionic nature of the dimer, we expect the stabilization arising from polyanionic BSA to decrease for A34F;D40N⁻³ and A34F;D40K⁻². The results match the predictions (Figure 2). Thus, decreasing the repulsion between the dimer and BSA, decreases the stabilization from polyanionic BSA.

If the A34F⁻⁴-lysozyme interaction is solely electrostatic, the A34F;D40N⁻³ and A34F;D40K⁻² proteins should restore the stability lost in A34F⁻⁴. However, the stabilities of all three complexes are equal within the uncertainty of the measurements (Table 1 and Figure 2). This observation shows that charge is not uniquely responsible for the destabilizing influence of lysozyme, consistent with studies of protein stability.^{30,41} The result can be rationalized because the surfaces of GB1 and lysozyme both possess hydrogen bond donors and acceptors capable of forming attractive interactions. Another important generalization is that electrostatic repulsions may overcome other sources of destabilization, but electrostatic attractions can reinforce only the inherent attractive interactions that exist between proteins and can lead to misfolding and disease.⁴²

Our data highlight the importance of the protein surface in controlling the strength of protein–protein interactions under physiologically relevant conditions. Manipulating the surface interactions between macromolecules resulted in changes on the order of 0.6 kcal/mol, the available thermal energy as defined by the product of the gas constant and the temperature (RT). In biology, small changes can lead to amazing effects. For instance, increasing the incubation temperature of alligator eggs by 4 °C, representing 0.01 kcal/mol of thermal energy, changes the sex of the hatchlings from 100% female to 100% male.⁴³ More importantly, we conducted our experiments at the highest concentration of protein cosolutes that provide high-quality spectra. These macromolecular concentrations are only one-third to one-sixth of the intracellular macromolecule concentration,^{2,3} and as we have shown,¹⁰ increasing the macromolecule concentration strengthens the influence of the interactions. Therefore, the charge effects we observe are probably more pronounced in cells. In summary, the spatial dependence of interactions based on protein charge and local pH suggests that manipulating chemical interactions provides a mechanism for regulating physiologically crucial events in the nonhomogeneous, crowded milieu of macromolecules that comprise the cellular interior.

Supplementary Material

Refer to Web version on PubMed Central for supplementary material.

Acknowledgments

Funding

Our research is supported by the National Science Foundation (MCB-1410854 and CHE-1607359) and the National Institutes of Health [NIGMS F31 GM126763 (to A.J.G.) and T32 GM008570] and was performed in facilities supported by the National Cancer Institute (P30 CA016086).

The authors thank the members of the Pielak lab for insightful discussions, Greg Young for assistance with NMR, and Thomas Boothby and Elizabeth Pielak for comments on the manuscript.

References

1. Ryan DP, Matthews JM. *Curr Opin Struct Biol.* 2005; 15:441–446. [PubMed: 15993577]
2. Zimmerman SB, Trach SO. *J Mol Biol.* 1991; 222:599–620. [PubMed: 1748995]
3. Theillet FX, Binolfi A, Frembgen-Kesner T, Hingorani K, Sarkar M, Kyne C, Li C, Crowley PB, Gierasch L, Pielak GJ, Elcock AH, Gershenson A, Selenko P. *Chem Rev.* 2014; 114:6661–6714. [PubMed: 24901537]
4. Sreere PA. *Annu Rev Biochem.* 1987; 56:89–124. [PubMed: 2441660]
5. Cohen RD, Pielak GJ. *Protein Sci.* 2017; 26:403–413. [PubMed: 27977883]
6. Vaĭnshteĭn BK. *Physics-Usppekhi.* 1973; 16:185.
7. Edelstein SJ. *Biophys J.* 1980; 32:347–360. [PubMed: 7248453]
8. McConkey EH. *Proc Natl Acad Sci U S A.* 1982; 79:3236–3240. [PubMed: 6954476]
9. Sarkar M, Li C, Pielak GJ. *Biophys Rev.* 2013; 5:187–194. [PubMed: 28510157]
10. Sarkar M, Smith AE, Pielak GJ. *Proc Natl Acad Sci U S A.* 2013; 110:19342–19347. [PubMed: 24218610]
11. Senske M, Törk L, Born B, Havenith M, Herrmann C, Ebbinghaus S. *J Am Chem Soc.* 2014; 136:9036–9041. [PubMed: 24888734]
12. Sarkar M, Lu J, Pielak GJ. *Biochemistry.* 2014; 53:1601–1606. [PubMed: 24552162]

13. Smith AE, Zhang Z, Pielak GJ, Li C. *Curr Opin Struct Biol.* 2015; 30:7–16. [PubMed: 25479354]
14. Danielsson J, Mu X, Lang L, Wang H, Binolfi A, Theillet FX, Bekei B, Logan DT, Selenko P, Wennerström H, Oliveberg M. *Proc Natl Acad Sci U S A.* 2015; 112:12402–12407. [PubMed: 26392565]
15. Gnutt D, Gao M, Brylski O, Heyden M, Ebbinghaus S. *Angew Chem, Int Ed.* 2015; 54:2548–2551.
16. Cohen RD, Pielak GJ. *J Am Chem Soc.* 2016; 138:13139–13142.
17. Cohen RD, Pielak GJ. *Protein Sci.* 2017; 26:1698–1703. [PubMed: 28571108]
18. Rivas G, Minton AP. *Trends Biochem Sci.* 2016; 41:970–981. [PubMed: 27669651]
19. Guseman AJ, Pielak GJ. *Biochemistry.* 2017; 56:971–976. [PubMed: 28102665]
20. Sukenik S, Ren P, Gruebele M. *Proc Natl Acad Sci U S A.* 2017; 114:6776–6781. [PubMed: 28607089]
21. Minton AP. *Biopolymers.* 1981; 20:2093–2120.
22. Minton AP. *Mol Cell Biochem.* 1983; 55:119–140. [PubMed: 6633513]
23. Ellis RJ. *Trends Biochem Sci.* 2001; 26:597–604. [PubMed: 11590012]
24. Ellis RJ, Hartl FU. *Curr Opin Struct Biol.* 1999; 9:102–110. [PubMed: 10047582]
25. Phillip Y, Sherman E, Haran G, Schreiber G. *Biophys J.* 2009; 97:875–885. [PubMed: 19651046]
26. Benton LA, Smith AE, Young GB, Pielak GJ. *Biochemistry.* 2012; 51:9773–9775. [PubMed: 23167542]
27. Sapir L, Harries D. *Curr Opin Colloid Interface Sci.* 2015; 20:3–10.
28. Crowley PB, Chow E, Papkovskaia T. *ChemBioChem.* 2011; 12:1043–1048. [PubMed: 21448871]
29. Wang Q, Zhuravleva A, Gierasch LM. *Biochemistry.* 2011; 50:9225–9236. [PubMed: 21942871]
30. Smith AE, Zhou LZ, Gorensen AH, Senske M, Pielak GJ. *Proc Natl Acad Sci U S A.* 2016; 113:1725–1730. [PubMed: 26755596]
31. Yu I, Mori T, Ando T, Harada R, Jung J, Sugita Y, Feig M. *eLife.* 2016; 5:e19274. [PubMed: 27801646]
32. Zhang N, An L, Li J, Liu Z, Yao L. *J Am Chem Soc.* 2017; 139:647–654. [PubMed: 28058828]
33. Kyne C, Crowley PB. *Biochemistry.* 2017; 56:5026–5032. [PubMed: 28832132]
34. Kyne C, Jordon K, Filoti DI, Laue TM, Crowley PB. *Protein Sci.* 2017; 26:258–267. [PubMed: 27813264]
35. Crowley PB, Brett K, Muldoon J. *ChemBioChem.* 2008; 9:685–688. [PubMed: 18260072]
36. Benton LA, Smith AE, Young GB, Pielak GJ. *Biochemistry.* 2012; 51:9773–9775. [PubMed: 23167542]
37. Monteith WB, Cohen RD, Smith AE, Guzman-Cisneros E, Pielak GJ. *Proc Natl Acad Sci U S A.* 2015; 112:1739–1742. [PubMed: 25624496]
38. Jee J, Byeon IJL, Louis JM, Gronenborn AM. *Proteins: Struct, Funct, Genet.* 2008; 71:1420–1431. [PubMed: 18076051]
39. Jee J, Ishima R, Gronenborn AM. *J Phys Chem B.* 2008; 112:6008–6012. [PubMed: 18004837]
40. Bava KA, Gromiha MM, Uedaira H, Kitajima K, Sarai A. *Nucleic Acids Res.* 2004; 32:D120–D121. [PubMed: 14681373]
41. Wang Y, Sarkar M, Smith AE, Krois AS, Pielak GJ. *J Am Chem Soc.* 2012; 134:16614–16618. [PubMed: 22954326]
42. Dobson CM. *Nature.* 2003; 426:884–890. [PubMed: 14685248]
43. Ferguson MWJ, Joanen T. *Nature.* 1982; 296:850–853. [PubMed: 7070524]

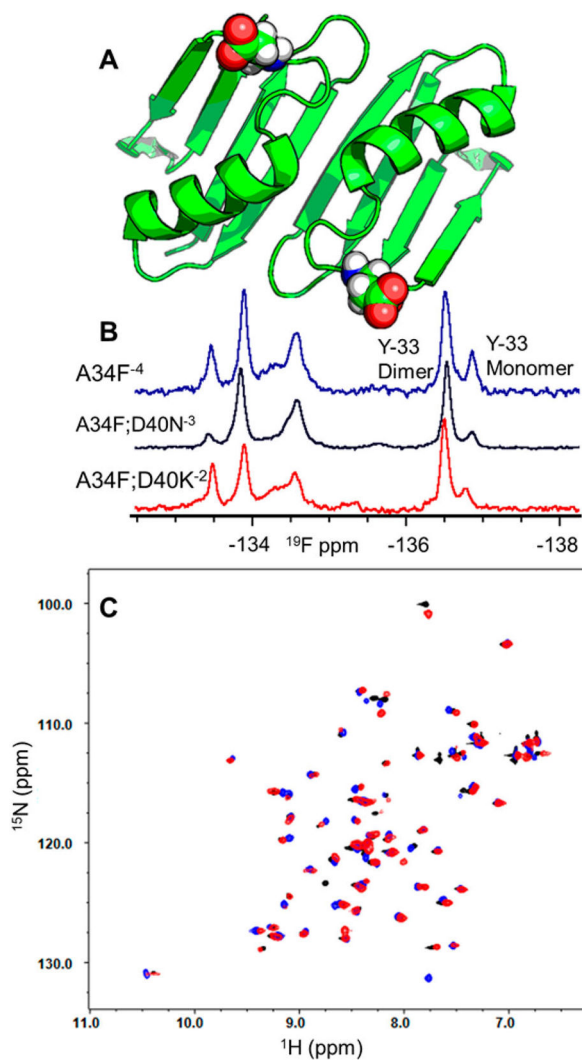


Figure 1.

(A) Dimer structure (Protein Data Bank entry 2RMM) with the atoms of residue 40 shown as spheres. (B) ^{19}F NMR spectra of A34F⁻⁴ (blue), A34F;D40N⁻³ (black), and A34F;D40K⁻² (red). (C) ^1H - ^{15}N HSQC spectra of the proteins using the same coloring as in panel B.

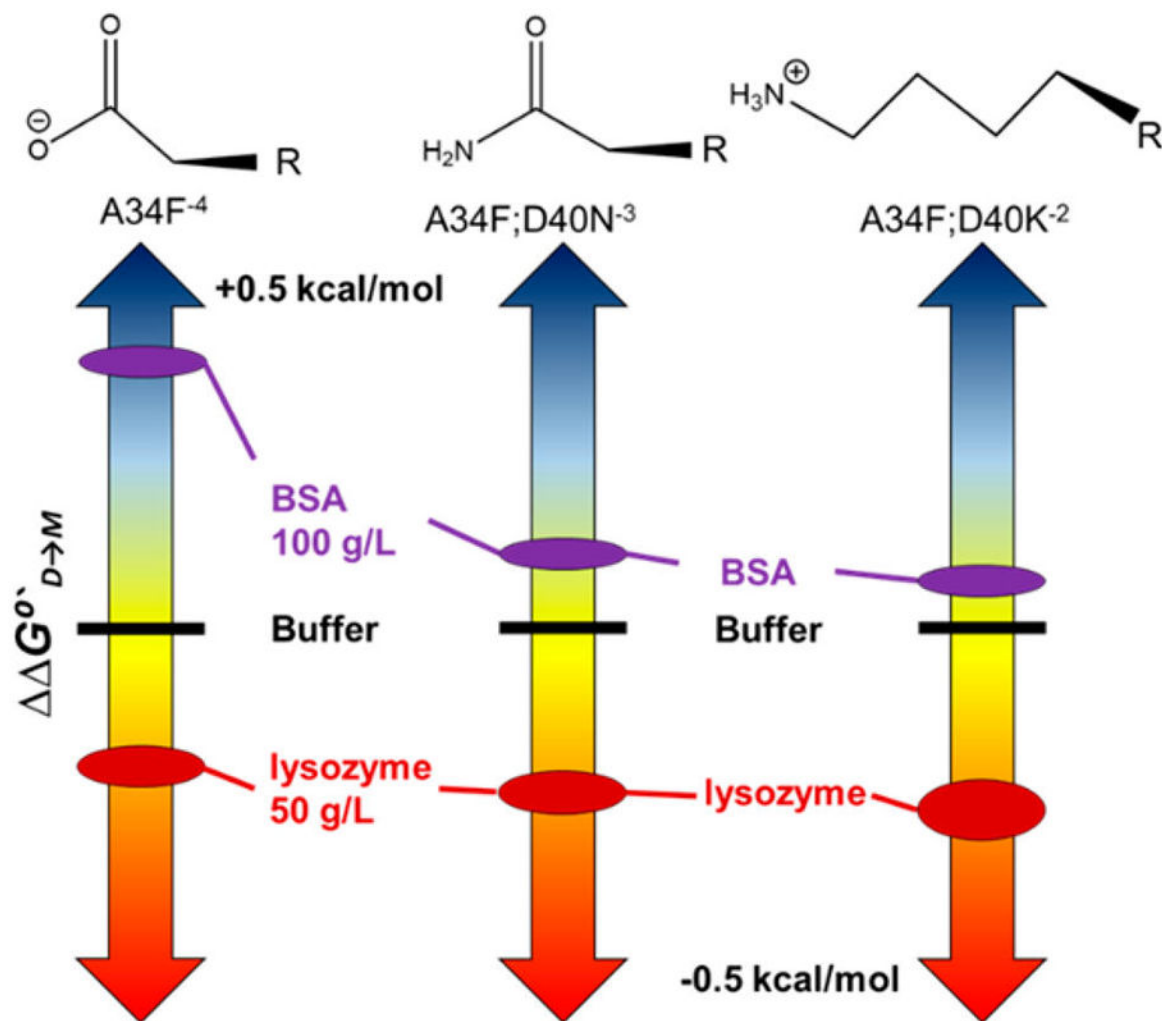


Figure 2. Side chains at position 40 and thermometer representations of $\Delta\Delta G^{\circ'}_{D \rightarrow M}$ (pH 7.5 and 298 K).

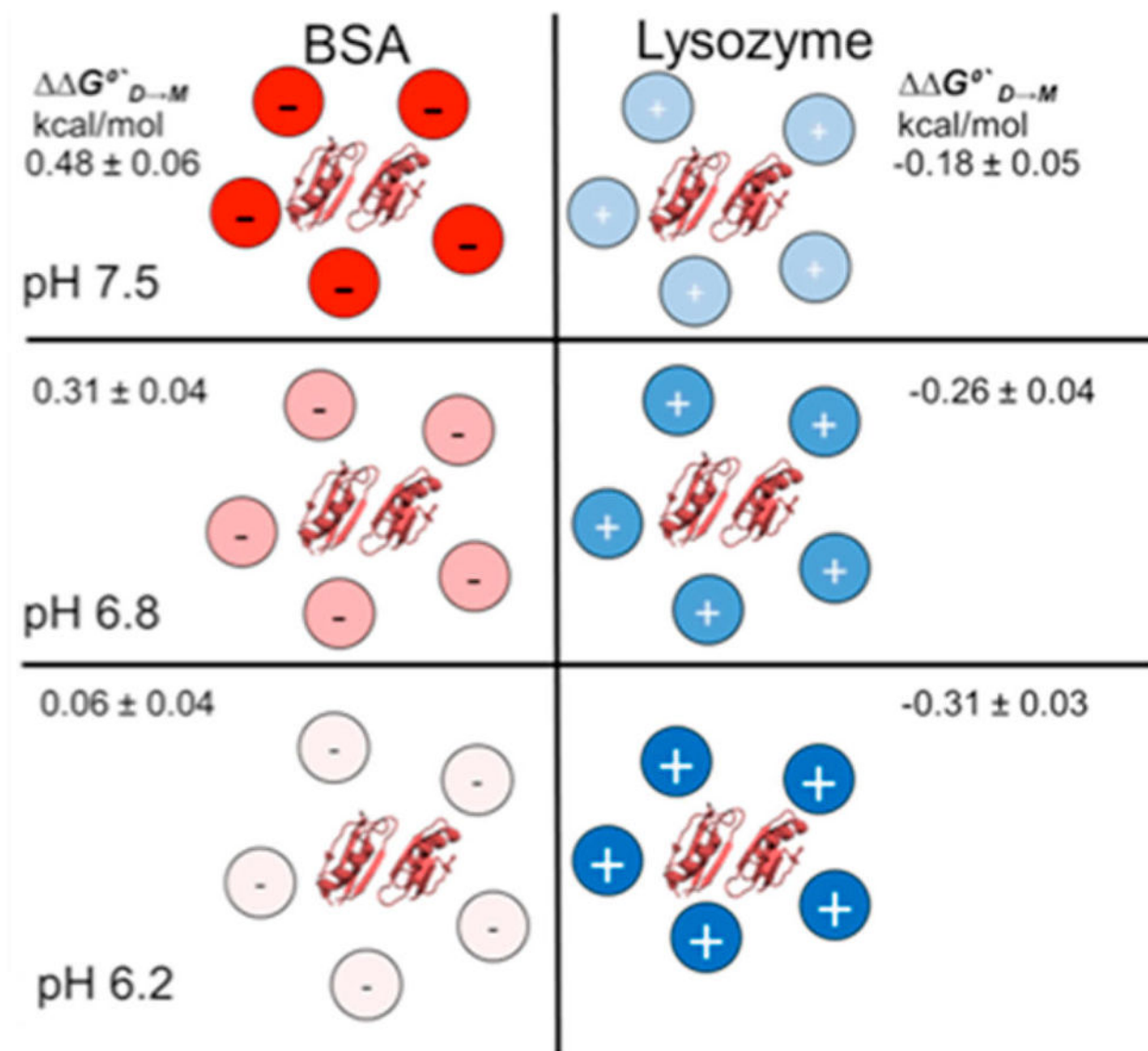


Figure 3. Graphical representations of A34F⁻⁴ dimerization in BSA and lysozyme at pH 7.5, pH 6.8, pH 6.2.

Table 1

Equilibrium Dissociation Parameters at 298 K

condition	$K_{D \rightarrow M}$ (μM)	$\Delta G_{D \rightarrow M}^{o'}$ (kcal/mol)	$\Delta \Delta G_{D \rightarrow M}^{o'}$ ^a (kcal/mol)
		A34F ⁻⁴ , pH 7.5 ^b	
buffer	59 ± 2	5.75 ± 0.03	N/A ^c
100 g/L BSA	26 ± 2	6.23 ± 0.05	0.48 ± 0.06
50 g/L lysozyme	80 ± 5	5.57 ± 0.04	-0.18 ± 0.05
		A34F ⁻⁴ , pH 6.8	
buffer	47 ± 2	5.88 ± 0.03	N/A ^c
BSA	28 ± 1	6.19 ± 0.02	0.31 ± 0.04
lysozyme	73 ± 2	5.62 ± 0.02	-0.26 ± 0.04
		A34F ⁻⁴ , pH 6.2	
buffer	39 ± 1	5.99 ± 0.02	N/A ^c
BSA	35 ± 2	6.05 ± 0.03	0.06 ± 0.04
lysozyme	66 ± 2	5.68 ± 0.02	-0.31 ± 0.03
		A34F;D40N ⁻³ , pH 7.5	
buffer	20 ± 1	6.38 ± 0.03	N/A ^c
BSA	16 ± 1	6.52 ± 0.04	0.13 ± 0.05
lysozyme	31 ± 2	6.13 ± 0.04	-0.26 ± 0.05
		A34F;D40K ⁻² , pH 7.5	
buffer	21 ± 2	6.36 ± 0.03	N/A ^c
BSA	18 ± 1	6.45 ± 0.03	0.09 ± 0.07
lysozyme	36 ± 3	6.04 ± 0.05	-0.32 ± 0.07

^aPositive values indicate stabilization. Uncertainties are reported as the standard deviation of the mean from triplicate analysis.

^bFrom ref 19.

^cNot applicable.